AJNR

Connectomic Basis for Tremor Control in Stereotactic Radiosurgical Thalamotomy

E.H. Middlebrooks, R.A. Popple, E. Greco, L. Okromelidze, H.C. Walker, D.A. Lakhani, A.R. Anderson, E.M. Thomas, H.D. Deshpande, B.A. McCullough, N.P. Stover, V.W. Sung, A.P. Nicholas, D.G. Standaert, T. Yacoubian, M.N. Dean, J.A. Roper, S.S. Grewal, M.T. Holland, J.N. Bentley, B.L. Guthrie and M. Bredel

AJNR Am J Neuroradiol published online 26 January 2023
http://www.ajnr.org/content/early/2023/01/25/ajnr.A7778

Published January 26, 2023 as 10.3174/ajnr.A7778

Connectomic Basis for Tremor Control in Stereotactic Radiosurgical Thalamotomy

E.H. Middlebrooks, R.A. Popple, E. Greco, L. Okromelidze, H.C. Walker, D.A. Lakhani, A.R. Anderson, E.M. Thomas, H.D. Deshpande, B.A. McCullough, N.P. Stover, V.W. Sung, A.P. Nicholas, D.G. Standaert, T. Yacoubian, M.N. Dean, J.A. Roper, S.S. Grewal, M.T. Holland, J.N. Bentley, B.L. Guthrie, and M. Bredel

ABSTRACT

BACKGROUND AND PURPOSE: Given the increased use of stereotactic radiosurgical thalamotomy and other ablative therapies for tremor, new biomarkers are needed to improve outcomes. Using resting-state fMRI and MR tractography, we hypothesized that a "connectome fingerprint" can predict tremor outcomes and potentially serve as a targeting biomarker for stereotactic radiosurgical thalamotomy.

MATERIALS AND METHODS: We evaluated 27 patients who underwent unilateral stereotactic radiosurgical thalamotomy for essential tremor or tremor-predominant Parkinson disease. Percentage postoperative improvement in the contralateral limb Fahn-Tolosa-Marin Clinical Tremor Rating Scale (TRS) was the primary end point. Connectome-style resting-state fMRI and MR tractography were performed before stereotactic radiosurgery. Using the final lesion volume as a seed, "connectivity fingerprints" representing ideal connectivity maps were generated as whole-brain R-maps using a voxelwise nonparametric Spearman correlation. A leave-one-out cross-validation was performed using the generated R-maps.

RESULTS: The mean improvement in the contralateral tremor score was 55.1% (SD, 38.9%) at a mean follow-up of 10.0 (SD, 5.0) months. Structural connectivity correlated with contralateral TRS improvement ($r = 0.52$; $P = .006$) and explained 27.0% of the variance in outcome. Functional connectivity correlated with contralateral TRS improvement ($r = 0.50$; $P = .008$) and explained 25.0% of the variance in outcome. Nodes most correlated with tremor improvement corresponded to areas of known network dysfunction in tremor, including the cerebello-thalamo-cortical pathway and the primary and extrastriate visual cortices.

CONCLUSIONS: Stereotactic radiosurgical targets with a distinct connectivity profile predict improvement in tremor after treatment. Such connectomic fingerprints show promise for developing patient-specific biomarkers to guide therapy with stereotactic radiosurgical thalamotomy.

ABBREVIATIONS: BOLD = blood oxygen level–dependent MRI; DBS = deep brain stimulation; DRTT = dentato-rubro-thalamic tract; SMS = simultaneous multislice; SRS = stereotactic radiosurgery; TRS = Fahn-Tolosa-Marin Clinical Tremor Rating Scale; VIM = ventral intermediate nucleus

Tremor is a debilitating neurologic condition that is seen with multiple disorders, most commonly in essential tremor and Parkinson's disease.[1] Patients who are refractory to pharmacologic therapies are potentially candidates for surgical intervention. Deep brain stimulation (DBS) is the current criterion standard surgical treatment; however, not all patients are candidates or wish to undergo DBS. Recently, there has been a resurgence in ablative therapies using incisionless ablative techniques such as stereotactic radiosurgery (SRS) and MR imaging–guided focused ultrasound. While ablative treatment mechanisms might overlap with DBS, little is known on the connectomics of SRS and tremor improvement.

In contrast to traditional "localizationist" models of the brain, a more recent shift to a network, or "connectomic," model has greatly enhanced our understanding of brain function and pathology.[2] Such a shift has also occurred in the realm of neuromodulation with recognition of many disorders as "circuitopathies"[3] and the need for targeted network surgery, or "connectomic surgery."[4] The connectomic model, using MR tractography as a measure of structural connectivity and resting-state fMRI as a measure of

Received September 8, 2022; accepted after revision December 30.

From the Departments of Radiology (E.H.M., E.G., L.O., D.A.L.) and Neurosurgery (E.H.M., S.S.G.), Mayo Clinic, Jacksonville, Florida; Departments of Radiation Oncology (R.A.P., A.R.A., E.M.T., M.B.), Neurology (H.C.W., B.A.M., N.P.S., V.W.S., A.P.N., D.G.S., T.Y., M.N.D.), Radiology (H.D.D.), and Neurosurgery (M.T.H., J.N.B., B.L.G.), University of Alabama at Birmingham, Birmingham, Alabama; Department of Radiology (D.A.L.), West Virginia University, Morgantown, West Virginia; Department of Radiation Oncology (E.M.T.), Ohio State University, Columbus, Ohio; and School of Kinesiology (J.A.R.), Auburn University, Auburn, Alabama.

This prospective clinical trial was funded by Varian Medical Systems Inc under the study protocol RAD 1601: EDGE Radiosurgery for Intractable Essential Tremor and Tremor-Dominant Parkinson's Disease (NCT03305588).

Please address correspondence to Erik H. Middlebrooks, MD, Department of Radiology, Mayo Clinic Florida, 4500 San Pablo Rd, Jacksonville, FL 32224; e-mail: Middlebrooks.Erik@mayo.edu; @EMiddlebrooksMD

Indicates article with online supplemental data.

http://dx.doi.org/10.3174/ajnr.A7778

functional connectivity, has been previously applied to better understand treatment effects in DBS surgery.[5-22] In treatment of tremor, this has led to the consolidation of the role of the cerebello-thalamo-cortical sensorimotor network in explaining many previously reported "sweet spots" in the DBS literature.[5-14]

To date, there has been limited application of the connectomic model to SRS in tremor. Using a combination of resting-state functional MR imaging and MR tractography, we explored whether the therapeutic network for SRS in treatment of tremor displays a "connectome fingerprint" that correlates with tremor improvement. Identification of such a network may provide further insight into the mechanism of tremor improvement and guide targeting in SRS. We also hypothesized that the similarity of any patient's individual connectivity map to the connectome fingerprint of tremor improvement will predict his or her measured tremor improvement, which may establish feasibility for the potential of connectivity fingerprints to guide SRS targeting.

MATERIALS AND METHODS

This prospective clinical trial was approved by the University of Alabama at Birmingham institutional review board. All patients gave verbal and written consent. The trial was registered at https://www.clinicaltrials.gov/ under trial NCT03305588. Subjects were recruited in collaboration with the University of Alabama at Birmingham Neurology, Neurosurgery, Movement Disorders, and Radiation Oncology Departments. Patients with medically refractory essential tremor or tremor-dominant Parkinson disease older than 18 years of age with Eastern Cooperative Oncology Group Performance Status of ≤2 were included. Patients were not candidates for DBS on the basis of either medical/surgical comorbidities or by their own choice. Patients were ineligible if they had prior brain radiosurgery or therapeutic brain radiation therapy or if there was a contraindication to MR imaging.

Imaging Protocol

Before thalamotomy, patients were scanned on a 3T Magnetom Prisma (Siemens) scanner with a high-performance, 80 mT/m gradient system and a 64-channel head/neck coil. Patients' heads were tightly packed in the head coil to minimize motion.

Diffusion imaging was obtained with a spin-echo EPI sequence using simultaneous multislice (SMS) excitation. A total of 64 diffusion directions were obtained with a b-value = 1500 s/mm^2 plus 6 B_0 volumes without diffusion-weighting. The diffusion scan was repeated with an opposing phase-encoding direction for distortion correction. Additional relevant parameters include TR = 3.3 seconds, TE = 90 ms, SMS factor = 4, in-plane acceleration = 2, phase partial Fourier = 6/8, receiver bandwidth = 1232 Hz/px, echo spacing = 0.94 ms, EPI factor = 140, in-plane resolution = 1.5 × 1.5 mm, section thickness = 1.5 mm, with scan time = 4 minutes and 21 seconds per acquisition.

A connectome-style resting-state fMRI was acquired with a multiecho blood oxygen level–dependent (BOLD) gradient-echo EPI sequence using SMS excitation. The temporal SNR of BOLD imaging is generally lower in subcortical regions due to many factors, including the distance from the receive coil and increased physiologic noise. To address this issue, we used a multiecho BOLD approach that significantly improves subcortical connectivity measures.[23] Additionally, the use of a reduced TR with high spatial resolution and a long, connectome-style BOLD acquisition has all been shown to improve the statistical analysis of resting-state fMRI data. Relevant parameters include the following: TR = 1.5 seconds, echo times = 12.4, 34.3, and 56.2 ms, flip angle = 65°, SMS factor = 4, in-plane acceleration = 2, phase partial Fourier = 6/8, receiver bandwidth = 1850 Hz/px, echo spacing = 0.66 ms, EPI factor = 81, in-plane resolution = 2.0 × 2.0 mm, section thickness = 2.0 mm. The scan was repeated with opposing phase-encoding directions to account for directional bias. A total of 1180 measurements were obtained with a total scan time of 31 minutes and 28 seconds.

A T1-weighted MPRAGE sequence was used for structural registration and performed before SRS. At 3 months after SRS, 3D T1-weighted images were repeated with intravenous contrast. See the Online Supplemental Data for sequence details.

SRS Procedure

Frameless SRS was performed using a thermoplastic mask with an open face molded to the patient's head. Plans were created using the Eclipse treatment planning system (Varian Medical Systems), and the dose was calculated using either the Analytical Anisotropic Algorithm or AcurosXB algorithm (Varian Eclipse Treatment Planning System) with grid spacing of 1 mm. Patients were treated using an Edge (Varian) linear accelerator equipped with a high-definition multileaf collimator and a 10 MV flattening-filter-free beam by using the virtual cone technique.[24] Optical surface guidance was used to monitor the patient position during treatment.[25] For full details of the procedure, see the Online Supplemental Data .

Clinical Testing

Before SRS, a baseline Fahn-Tolosa-Marin Clinical Tremor Rating Scale (TRS) was assessed. The TRS was repeated at each follow-up assessment after SRS, and the last documented TRS score was used for analysis. TRS was assessed by a single examiner who was blinded to the imaging results at the time of assessment. The primary outcome measure for the study was a percentage decrease in contralateral upper and lower body tremors, measured as the sum of the lateralized TRS scores from Part I on the body side opposite of the treatment hemisphere. Any disease-related medications were maintained at preoperative doses for follow-up.

Image Preprocessing

The postoperative postcontrast T1-weighted images were coregistered to the preoperative T1-weighted images using Advanced Normalization Tools (http://stnava.github.io/ANTs/). The final lesion location was manually segmented as the enhancing region on the 3-month postoperative postcontrast T1-weighted images.

The diffusion data underwent eddy current correction, section-to-volume movement correction, and outlier replacement in FSL "eddy_cuda" (https://git.fmrib.ox.ac.uk/fsl/conda/fsl-eddy-cuda) on a custom-built Linux workstation using 3 NVIDIA Quadro P5000 GPUs. Susceptibility-induced distortions were corrected with FSL "topup" (https://fsl.fmrib.ox.ac.uk/fsl/fslwiki/topup) using the repeat acquisitions in opposing phase-encoding directions.[26] FSL "BEDPOSTX_GPU" (https://users.fmrib.ox.ac.

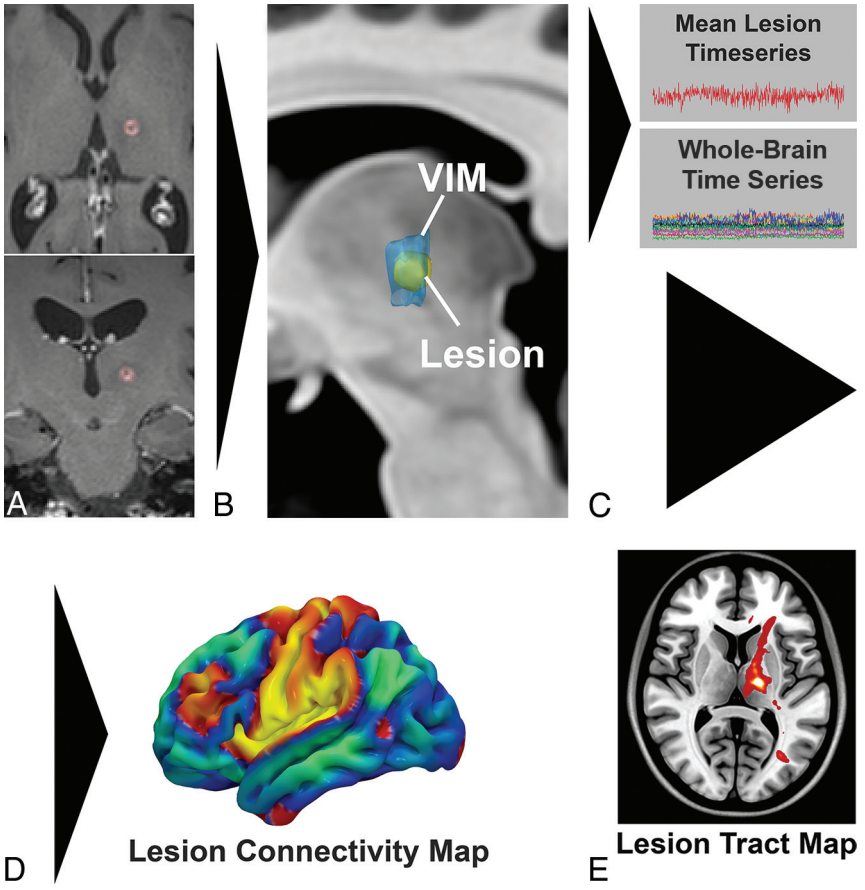

FIG 1. Pipeline for generation of a single-subject lesion connectivity map and lesion tract map (*A* and *B*). The lesion is segmented from the posttreatment MR imaging (*C*). The mean BOLD timeseries for the lesion is extracted and correlated to all other brain voxels. *D*, The resulting *t*-score map is a patient-specific lesion connectivity map. *E*, The lesion is used as a seed region to generate a patient-specific lesion tract map representing the probability of all streamlines connected to the lesion.

uk/~moisesf/Bedpostx_GPU/) was used to estimate the orientation distribution functions with 3 fiber orientations modeled per voxel. The diffusion data were coregistered to the T1 MPRAGE using a boundary-based registration implemented in FreeSurfer (http://surfer.nmr.mgh.harvard.edu). An exclusion mask was generated to include the ventricles and contralateral hemisphere white matter.

The multiecho BOLD data were initially preprocessed in AFNI, Version 22.0.06 (https://afni.nimh.nih.gov/). Preprocessing steps included realignment, spatial smoothing of 4-mm full width at half maximum, and coregistration to the T1 MPRAGE. Denoising of the data was performed with multiecho independent component analysis using TE-dependent analysis implemented in AFNI. Last, motion censoring (framewise displacement of >0.3 mm) and outlier detection were performed using default values in AFNI. Global mean signal regression and regression of motion parameters were also performed.

Connectome Generation

Probabilistic tractography was performed using "probtrackx2_gpu" (https://users.fmrib.ox.ac.uk/~moisesf/Probtrackx_GPU/index.html) from the FMRIB Software Library, Version 6.0.3 (http://fsl.fmrib.ox.ac.uk) in each of the subjects, with 250,000 samples, a curvature threshold of 0.2, modified Euler streamlining (https://mycareerwise.com/programming/category/numerical-analysis/modified-euler-method), and a step length of 0.5 mm. A region-of-avoidance was added to exclude the internal capsule and deep white matter of the contralateral hemisphere. Because no plausible fibers or existing evidence implicates tracts connecting the thalamus with the contralateral hemisphere via the capsular fibers, such connections are most likely spurious fibers and their inclusion leads to an artificial increase in directions of freedom with resulting inflation of *P* values. Probabilistic tractography was performed using the segmented lesion as the seed region to generate "lesion tract maps" of all tracts passing through the lesion (Fig 1).

The preprocessed BOLD resting-state fMRI data underwent a seed-based correlation analysis across the entire brain for each subject using the segmented lesion as the seed point to generate a whole-brain "lesion connectivity map" (Fig 1). The resulting t-maps were used for subsequent analysis.

The structural images, lesion connectivity maps, and lesion tract maps were then normalized into Montreal Neurological Institute template space, as described in the Online Supplemental Data. The right hemisphere lesion connectivity maps and lesion tract maps were nonlinearly flipped to the left hemisphere for comparison across the cohort.

Connectome Analysis

To determine the relationship between structural connectivity and contralateral tremor improvement, we generated an ideal tract fingerprint for the cohort. First, the individual lesion tract maps for each subject were correlated with percentage improvement in the contralateral tremor to generate a Spearman rank-correlation coefficient on a voxel-by-voxel basis. The resultant group R-map, or tract fingerprint, represents an optimal voxel-by-voxel tract map for contralateral tremor improvement.

To assess the significance of the tract fingerprint in predicting outcomes, we performed a leave-one-out cross-validation. An R-map was created by correlating tracts traversing the lesion with the contralateral TRS improvement using all patients except one, withheld for validation. The probabilistic tract map from the left-out patient was then used to calculate spatial similarity (measured via the Fisher z-transformed spatial correlation coefficient) with the tract fingerprint generated from the remainder of the cohort. The similarity index for each left-out subject was then correlated

Demographic and clinical outcome data

Criteria	
Age at treatment (yr)	72.3 (SD, 13.1)
Male sex (No.) (%)	17 (63.0%)
Essential tremor (No.) (%)	22 (81.5%)
Parkinson disease (No.) (%)	4 (14.8%)
ET + PD (No.) (%)	1 (3.7%)
Baseline contralateral TRS score (mean)	6.8 (SD, 4.3)
Baseline ipsilateral TRS score (mean)	4.9 (SD, 4.3)
Baseline midline TRS score (mean)	2.5 (SD, 2.8)
Follow-up duration (mean) (mo)	10.0 (SD, 5.0)
Postoperative contralateral TRS improvement (mean)	55.1% (SD, 38.9%)
Postoperative ipsilateral TRS improvement (mean)	9.9% (SD, 61.8%)
Postoperative midline TRS improvement (mean)	27.2% (SD, 90.0%)

Note:—ET indicates essential tremor; PD, Parkinson disease.

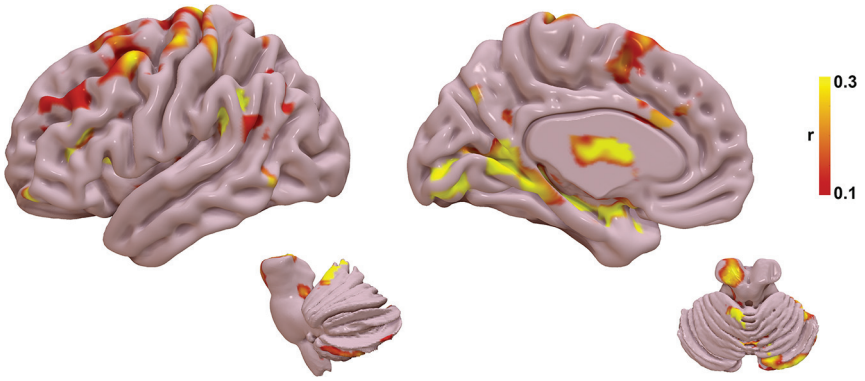

FIG 2. Tract fingerprint representing the ideal tract connectivity pattern for tremor improvement. Commonly implicated areas of abnormality in tremor are identified, including the cerebello-thalamo-cortical motor network, as well as striate and extrastriate cortical regions.

versus the measured tremor improvement using the Spearman correlation.

Next, the process was repeated using the lesion connectivity map generated from the resting-state fMRI for each individual subject to create a functional fingerprint.

Statistics

Demographic data were expressed as mean, range, and SD, as appropriate. The primary outcome measure was the percentage change in the contralateral TRS. Correlation of lesion volume and contralateral TRS improvement was assessed with a nonparametric Spearman correlation. Statistical significance was considered as $P < .05$.

RESULTS

Demographic and Clinical Results

Forty total patients were enrolled in the clinical trial. Three died of unrelated causes before follow-up, 1 declined treatment, 3 patients were not eligible for 3T MR imaging, and 6 patients were lost to follow-up for their imaging and/or clinical assessment, leaving 27 patients for analysis. Demographic and group outcome data are listed in the Table. Twenty-three (85.2%) patients underwent left thalamotomy, while 4 (14.8%) had right thalamotomy. Twenty patients (74.0%) had a ≥50% reduction in contralateral tremor, while 7 patients (26.0%) had <50% reduction in contralateral tremor. The mean improvement in the contralateral tremor score was 55.1% (SD, 38.9%). All patients had at least 6 months of clinical follow-up with the mean duration of follow-up being 10.0 (SD, 5.0) months. Adverse events determined to be related to radiosurgery included 1 subject with grade I sensory deficits consisting of numbness in the left first and second digits and left-sided mouth and buccal mucosa dysesthesia occurring 10 months after radiosurgery. Two subjects experienced grade II radiation necrosis consistent with hyper-response. One of these subjects experienced right-foot drag, right-hand grip weakness, right-arm proprioceptive loss, mild expressive aphasia, bilateral lip paresthesia, and left-sided headache occurring 7 months after radiosurgery. One subject experienced falls, dysarthria, right-arm and right-leg weakness, and incoordination occurring 11 months after radiosurgery. Both subjects with grade II radionecrosis reported near-resolution of tremor at 4 months after radiosurgery. All 3 subjects with radiosurgery-related adverse events were treated with tapered corticosteroids and bevacizumab infusions. There were no grade III–V adverse events related to radiosurgery.

Structural Connectome Analysis

The tract R-map, or tract fingerprint, is shown in Fig 2. The cerebello-thalamo-cortical somatosensory network is a primary component of the affected network, including the primary somatosensory cortex, supplementary motor area, premotor cortex, ventral thalamic nuclei, and cerebellum—primarily cerebellar lobules IV, V, VI, and VIIIB, all areas implicated in the cerebellar somatosensory network.[27] Additional connectivity to temporal, occipital, and prefrontal areas is also present. The tract pathways correlated to tremor improvement (Fig 3) show primary involvement of the dentato-rubro-thalamic tract (DRTT); thalamocortical tracts to the primary sensorimotor, supplementary motor area, and prefrontal cortex; as well as the pallidothalamic tracts.

Results of the leave-one-out cross-validation of the tractography are shown in Fig 4*A*. The structural connectivity correlated with measured improvement in contralateral TRS ($r = 0.52$; $P = .006$) and could explain 27.0% of the variance in outcome.

Functional Connectome Analysis

The functional R-map, or functional fingerprint, is shown in Fig 5. The functional connectivity data further corroborate the structural connectivity, showing a correlation with cerebello-thalamo-cortical

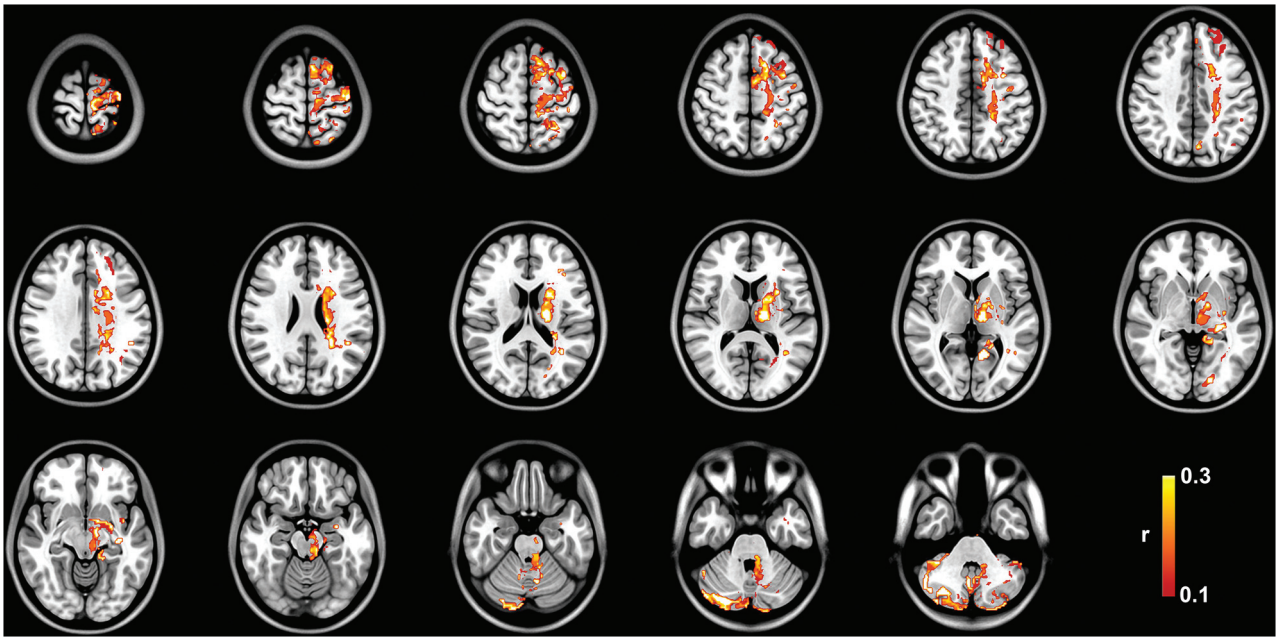

FIG 3. Group tract R-map of pathways most correlated with tremor improvement.

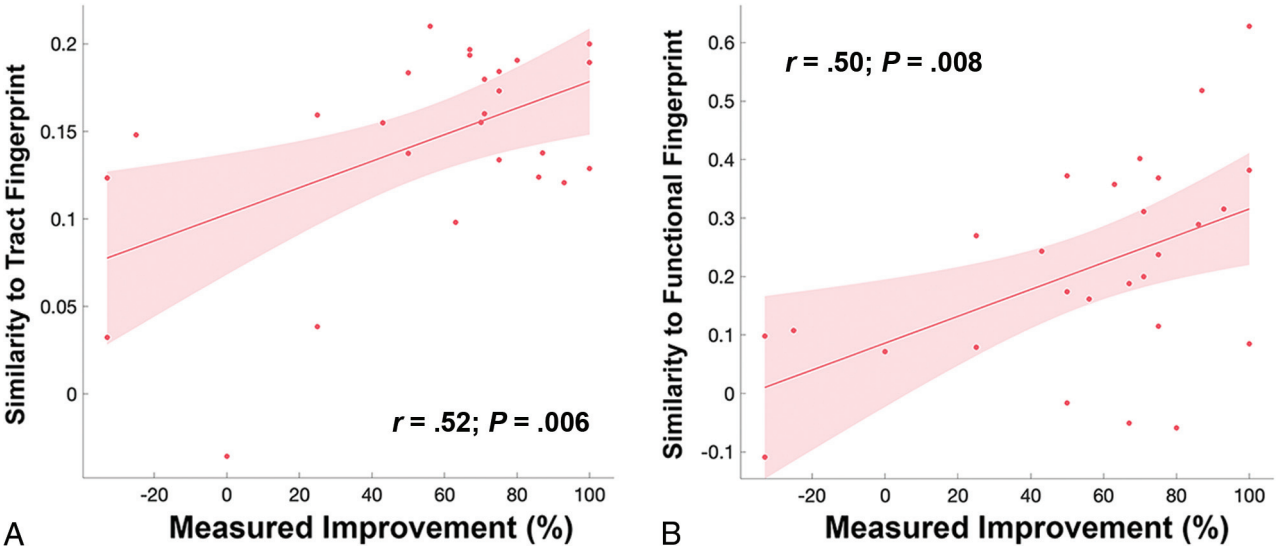

FIG 4. *A*, Leave-one-out cross-validation of the tract fingerprint shows greater similarity of the individual's lesion tract map to the fingerprint map predicted measured improvement in tremor ($r = 0.52$; $P = .006$). *B*, Leave-one-out cross-validation of the functional fingerprint also shows that greater similarity of the individual's lesion functional map to the fingerprint map predicted measured improvement in tremor ($r = 0.50$; $P = .008$).

somatosensory network, in particular the primary somatosensory cortex, ventral thalamic nuclei, and cerebellar lobules IV, V, VI, and VIIIB. Additional connectivity to temporal, occipital, and prefrontal areas is also present. Results for the leave-one-out cross-validation of the functional connectivity are shown in Fig 4*B*. The functional connectivity correlated with measured improvement in contralateral TRS ($r = 0.50$; $P = .008$) and could explain 25.0% of the variance in outcome.

DISCUSSION

In this study, we show that improvement in tremor after SRS thalamotomy is significantly correlated with a distinct pattern of structural and functional connectivity, primarily via the cerebello-thalamo-cortical pathway. This network has been previously demonstrated to be an important driver in tremor pathophysiology and a target for other forms of neuromodulation, such as DBS. Our findings indicate that a significant amount of variance in tremor outcomes after SRS are driven by an identifiable network topology, which may serve as a new therapeutic biomarker for SRS targeting. As opposed to other forms of neuromodulation, such as DBS, there are no intraprocedural biomarkers to validate target selection in SRS. By application of the concept of connectomic surgery,[12] we have shown the potential of a lesion connectome fingerprint to predict tremor improvement from a given SRS target using both MR tractography and resting-state fMRI.

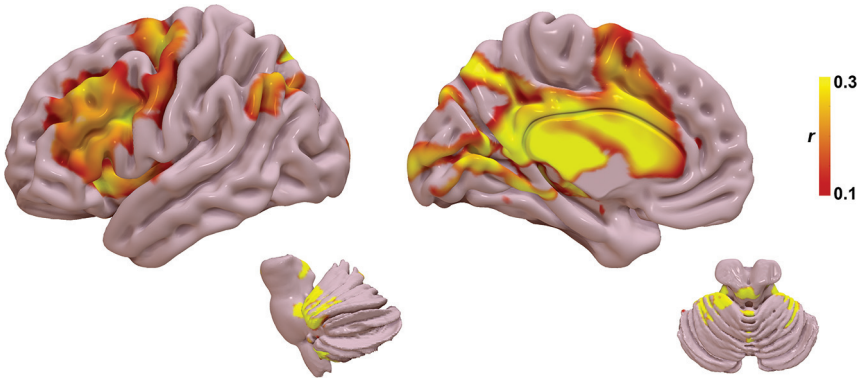

FIG 5. Functional fingerprint representing the ideal tract connectivity pattern for tremor improvement. Similar to the tract fingerprint, commonly implicated areas of abnormality in tremor are identified, including the cerebello-thalamo-cortical motor network as well as the striate and extrastriate cortical regions.

Our approach may enhance network-specific targeting in SRS and provide patient-specific biomarkers.

The optimal target for neuromodulation of tremor has been debated for decades. Most commonly proposed targets have been the ventral intermediate nucleus (VIM) and the posterior subthalamic area, including the caudal zona incerta, prelemniscal radiations, and subthalamic nucleus.[11] More recently, connectivity studies in DBS have suggested that these targets are unified by a common network and all targets overlap with the DRTT.[7,14] The role of the DRTT in tremor improvement has been well-demonstrated in DBS,[5-14,28-34] but limited data exist on the use of tractography in surgical planning for SRS.[35,36] Historically, the DRTT is defined by efferent cerebellar fibers originating in the dentate nucleus of the cerebellum that traverse superiorly through the ipsilateral superior cerebellar peduncle, decussate in the midbrain, pass the red nucleus (but without synapsing in the red nucleus), en route to the contralateral VIM and posterior vetralis oralis nucleus.[37,38] Tracts ultimately reach the contralateral primary motor cortex and premotor/supplementary motor cortex from the VIM and vetralis oralis nucleus, respectively. More recently, a small number of DRTT fibers have been shown to follow a similar path but without decussation in the midbrain and extend to the ipsilateral thalamus; however, these tracts likely have less of a role in motor function.[37,38] Our study adds further evidence to the role of the DRTT in the surgical treatment of tremor, particularly implicating a similar therapeutic target in SRS as seen in DBS.

From an anatomic perspective, nodes within the fingerprint maps correspond to areas known to exhibit network abnormalities in tremor. First, the fingerprint network distribution agrees with established network abnormalities attributed to the development of tremor via tremor-specific frequency synchronization within multiple nodes in the cerebello-thalamo-cortical pathway, including the cerebellum, thalamus, primary sensorimotor cortex, supplementary motor cortex, and premotor cortex.[39,40] Similar to prior work in DBS for essential tremor, we found that a lesion network fingerprint that includes the motor and supplementary motor networks also correlates with tremor improvement in SRS.[7,14] Additionally, there was correlation with cerebellar lobules IV, V, and VI, which are regions previously shown to be abnormal in essential tremor and part of the sensorimotor network.[41] Taken together, our results suggest that the therapeutic network involved in SRS thalamotomy provides evidence for targeting biomarkers similar to those in the existing DBS literature.

Most interesting, we also found structural and functional connectivity to the primary and extrastriate visual cortex as part of the tremor connectome fingerprint. While not historically considered a major part of tremor pathogenesis, the primary and associative visual cortices have been the subject of more recent investigation of the role of the visuospatial network in tremor augmentation. Archer et al[42] showed that visual feedback exacerbates tremor severity in essential tremor and functional changes in extrastriate areas correlate with the worsening of tremor. Likewise, postsurgical alterations in brain connectivity have been observed in the visual cortex that correlated with tremor improvement in MR imaging–guided focused ultrasound[43] and SRS;[44] however, direct activation of this region was not observed with active DBS.[45] Pretreatment functional connectivity between the ventrolateral thalamus and visual association areas has also been shown as a predictor of tremor improvement after SRS.[46] Further studies are needed to understand the true causal effect of visual network connectivity versus a coincident change in addition to the cerebello-thalamo-cortical motor network.

Several limitations to our study are noteworthy. Although tremor outcomes were gathered prospectively, the connectomics analyses were applied in retrospect. Thus, future studies would benefit from examining the effects of prospective targeting based on the proposed biomarkers. SRS thalamotomy was effective for tremor and well-tolerated overall. Larger cohorts, however, are needed to expand on these results and better assess the frequency of potential adverse effects. Additionally, intersubject variations in the temporal evolution of the lesion may result in fluctuation of the clinical response and are relatively unpredictable pre-SRS. We chose to use the 3-month post-SRS examination because this was thought to most accurately represent the intended target location with less variability among patients. Last, there are inherent limitations to MR tractography and resting-state fMRI that have been well-described.[6,31,47] We used a robust probabilistic tracking approach and a lengthy fMRI acquisition to increase the robustness of our connectome modeling; however, these protocols may be challenging to implement in routine clinical care, and further studies will be needed to explore reproducibility with less robust data sets.

CONCLUSIONS

Using a connectomic approach, we have shown that SRS targets with a distinct connectivity profile predict posttreatment tremor improvement. Among these are networks implicated in tremor pathogenesis, including the cerebello-thalamo-cortical network

and visual networks. The use of such connectomic fingerprints may provide a patient-specific biomarker for SRS thalamotomy; however, validation of this approach for use in targeting will require further studies to prospectively validate these results.

Disclosure forms provided by the authors are available with the full text and PDF of this article at www.ajnr.org.

REFERENCES

1. Louis ED, Ferreira JJ. **How common is the most common adult movement disorder? Update on the worldwide prevalence of essential tremor.** *Mov Disord* 2010;25:534–41 CrossRef Medline
2. Sporns O, Tononi G, Kötter R. **The human connectome: a structural description of the human brain.** *PLoS Comput Biol* 2005;1:e42 CrossRef Medline
3. Lozano AM, Lipsman N. **Probing and regulating dysfunctional circuits using deep brain stimulation.** *Neuron* 2013;77:406–24 CrossRef Medline
4. Henderson JM. **"Connectomic surgery": diffusion tensor imaging (DTI) tractography as a targeting modality for surgical modulation of neural networks.** *Front Integr Neurosci* 2012;6:15 CrossRef Medline
5. Middlebrooks EH, Domingo RA, Vivas-Buitrago T, et al. **Neuroimaging advances in deep brain stimulation: review of indications, anatomy, and brain connectomics.** *AJNR Am J Neuroradiol* 2020;41:1558–68 CrossRef Medline
6. Middlebrooks EH, Okromelidze L, Carter RE, et al. **Directed stimulation of the dentato-rubro-thalamic tract for deep brain stimulation in essential tremor: a blinded clinical trial.** *Neuroradiol J* 2022;35:203–12 CrossRef Medline
7. Middlebrooks EH, Okromelidze L, Wong JK, et al. **Connectivity correlates to predict essential tremor deep brain stimulation outcome: evidence for a common treatment pathway.** *Neuroimage Clin* 2021;32:102846 CrossRef Medline
8. Middlebrooks EH, Tuna IS, Almeida L, et al. **Structural connectivity-based segmentation of the thalamus and prediction of tremor improvement following thalamic deep brain stimulation of the ventral intermediate nucleus.** *Neuroimage Clin* 2018;20:1266–73 CrossRef Medline
9. Neudorfer C, Kroneberg D, Al-Fatly B, et al. **Personalizing deep brain stimulation using advanced imaging sequences.** *Ann Neurol* 2022;91:613–28 CrossRef Medline
10. Tsuboi T, Wong JK, Eisinger RS, et al. **Comparative connectivity correlates of dystonic and essential tremor deep brain stimulation.** *Brain* 2021;144:1774–86 CrossRef Medline
11. Wong JK, Hess CW, Almeida L, et al. **Deep brain stimulation in essential tremor: targets, technology, and a comprehensive review of clinical outcomes.** *Expert Rev Neurother* 2020;20:319–31 CrossRef Medline
12. Wong JK, Middlebrooks EH, Grewal SS, et al. **A comprehensive review of brain connectomics and imaging to improve deep brain stimulation outcomes.** *Mov Disord* 2020;35:741–51 CrossRef Medline
13. Wong JK, Patel B, Middlebrooks EH, et al. **Connectomic analysis of unilateral dual-lead thalamic deep brain stimulation for treatment of multiple sclerosis tremor.** *Brain Commun* 2022;4:fcac063 CrossRef Medline
14. Al-Fatly B, Ewert S, Kubler D, et al. **Connectivity profile of thalamic deep brain stimulation to effectively treat essential tremor.** *Brain* 2019;142:3086–98 CrossRef Medline
15. Middlebrooks EH, Grewal SS, Stead M, et al. **Differences in functional connectivity profiles as a predictor of response to anterior thalamic nucleus deep brain stimulation for epilepsy: a hypothesis for the mechanism of action and a potential biomarker for outcomes.** *Neurosurg Focus* 2018;45:E7 CrossRef Medline
16. Middlebrooks EH, He X, Grewal SS, et al. **Neuroimaging and thalamic connectomics in epilepsy neuromodulation.** *Epilepsy Res* 2022;182:106916 CrossRef Medline
17. Middlebrooks EH, Jain A, Okromelidze L, et al. **Acute brain activation patterns of high- versus low-frequency stimulation of the anterior nucleus of the thalamus during deep brain stimulation for epilepsy.** *Neurosurgery* 2021;89:901–08 CrossRef Medline
18. Middlebrooks EH, Lin C, Okromelidze L, et al. **Functional activation patterns of deep brain stimulation of the anterior nucleus of the thalamus.** *World Neurosurg* 2020;136:357–63.e2 CrossRef Medline
19. Tsuboi T, Charbel M, Peterside DT, et al. **Pallidal connectivity profiling of stimulation-induced dyskinesia in Parkinson's disease.** *Mov Disord* 2021;36:380–88 CrossRef Medline
20. Horn A, Reich M, Vorwerk J, et al. **Connectivity predicts deep brain stimulation outcome in Parkinson disease.** *Ann Neurol* 2017;82:67–78 CrossRef Medline
21. Li N, Baldermann JC, Kibleur A, et al. **A unified connectomic target for deep brain stimulation in obsessive-compulsive disorder.** *Nat Commun* 2020;11:3364 CrossRef Medline
22. Reich MM, Horn A, Lange F, et al. **Probabilistic mapping of the antidystonic effect of pallidal neurostimulation: a multicentre imaging study.** *Brain* 2019;142:1386–98 CrossRef Medline
23. Kundu P, Inati SJ, Evans JW, et al. **Differentiating BOLD and non-BOLD signals in fMRI time series using multi-echo EPI.** *Neuroimage* 2012;60:1759–70 CrossRef Medline
24. Popple RA, Wu X, Brezovich IA, et al. **The virtual cone: a novel technique to generate spherical dose distributions using a multileaf collimator and standardized control-point sequence for small target radiation surgery.** *Adv Radiat Oncol* 2018;3:421–30 CrossRef Medline
25. Li G, Ballangrud A, Kuo LC, et al. **Motion monitoring for cranial frameless stereotactic radiosurgery using video-based three-dimensional optical surface imaging.** *Med Phys* 2011;38:3981–94 CrossRef Medline
26. Graham MS, Drobnjak I, Jenkinson M, et al. **Quantitative assessment of the susceptibility artefact and its interaction with motion in diffusion MRI.** *PLoS One* 2017;12:e0185647 CrossRef Medline
27. Buckner RL, Krienen FM, Castellanos A, et al. **The organization of the human cerebellum estimated by intrinsic functional connectivity.** *J Neurophysiol* 2011;106:2322–45 CrossRef Medline
28. Middlebrooks EH, Grewal SS, Holanda VM. **Complexities of connectivity-based DBS targeting: rebirth of the debate on thalamic and subthalamic treatment of tremor.** *Neuroimage Clin* 2019;22:101761 CrossRef Medline
29. Middlebrooks EH, Tipton P, Okromelidze L, et al. **Deep brain stimulation for tremor: direct targeting of a novel imaging biomarker.** *Ann Neurol* 2022;92:341–42 CrossRef Medline
30. Neudorfer C, Kroneberg D, Al-Fatly B, et al. **Reply to "Deep Brain Stimulation for Tremor: Direct Targeting of a Novel Imaging Biomarker."** *Ann Neurol* 2022;92:343–44 CrossRef Medline
31. Akram H, Dayal V, Mahlknecht P, et al. **Connectivity derived thalamic segmentation in deep brain stimulation for tremor.** *Neuroimage Clin* 2018;18:130–42 CrossRef Medline
32. Coenen VA, Allert N, Paus S, et al. **Modulation of the cerebello-thalamo-cortical network in thalamic deep brain stimulation for tremor: a diffusion tensor imaging study.** *Neurosurgery* 2014;75:657–69; discussion 6697–70 CrossRef Medline
33. Coenen VA, Sajonz B, Prokop T, et al. **The dentato-rubro-thalamic tract as the potential common deep brain stimulation target for tremor of various origin: an observational case series.** *Acta Neurochir (Wien)* 2020;162:1053–66 CrossRef Medline
34. Coenen VA, Varkuti B, Parpaley Y, et al. **Postoperative neuroimaging analysis of DRT deep brain stimulation revision surgery for complicated essential tremor.** *Acta Neurochir (Wien)* 2017;159:779–87 CrossRef Medline
35. Kim W, Chivukula S, Hauptman J, et al. **Diffusion tensor imaging-based thalamic segmentation in deep brain stimulation for chronic pain conditions.** *Stereotact Funct Neurosurg* 2016;94:225–34 CrossRef Medline
36. Kim W, Sharim J, Tenn S, et al. **Diffusion tractography imaging-guided frameless linear accelerator stereotactic radiosurgical**

thalamotomy for tremor: case report. *J Neurosurg* 2018;128:215–21 CrossRef Medline
37. Gallay MN, Jeanmonod D, Liu J, et al. **Human pallidothalamic and cerebellothalamic tracts: anatomical basis for functional stereotactic neurosurgery.** *Brain Struct Funct* 2008;212:443–63 CrossRef Medline
38. Petersen KJ, Reid JA, Chakravorti S, et al. **Structural and functional connectivity of the nondecussating dentato-rubro-thalamic tract.** *Neuroimage* 2018;176:364–71 CrossRef Medline
39. Hellwig B, Haussler S, Schelter B, et al. **Tremor-correlated cortical activity in essential tremor.** *Lancet* 2001;357:519–23 CrossRef Medline
40. McAuley JH, Marsden CD. **Physiological and pathological tremors and rhythmic central motor control.** *Brain* 2000;123:1545–67 CrossRef
41. Nicoletti V, Cecchi P, Pesaresi I, et al. **Cerebello-thalamo-cortical network is intrinsically altered in essential tremor: evidence from a resting state functional MRI study.** *Sci Rep* 2020;10:16661 CrossRef Medline
42. Archer DB, Coombes SA, Chu WT, et al. **A widespread visually-sensitive functional network relates to symptoms in essential tremor.** *Brain* 2018;141:472–85 CrossRef Medline
43. Xiong Y, Han D, He J, et al. **Correlation of visual area with tremor improvement after MRgFUS thalamotomy in Parkinson's disease.** *J Neurosurg* 2022;136:681–88 CrossRef Medline
44. Tuleasca C, Najdenovska E, Regis J, et al. **Clinical response to VIM's thalamic stereotactic radiosurgery for essential tremor is associated with distinctive functional connectivity patterns.** *Acta Neurochir (Wien)* 2018;160:611–24 CrossRef Medline
45. Gibson WS, Jo HJ, Testini P, et al. **Functional correlates of the therapeutic and adverse effects evoked by thalamic stimulation for essential tremor.** *Brain* 2016;139:2198–210 CrossRef Medline
46. Tuleasca C, Najdenovska E, Régis J, et al. **Pretherapeutic motor thalamus resting-state functional connectivity with visual areas predicts tremor arrest after thalamotomy for essential tremor: tracing the cerebello-thalamo-visuo-motor network.** *World Neurosurg* 2018;117:e438–49 CrossRef Medline
47. Schlaier JR, Beer AL, Faltermeier R, et al. **Probabilistic vs. deterministic fiber tracking and the influence of different seed regions to delineate cerebellar-thalamic fibers in deep brain stimulation.** *Eur J Neurosci* 2017;45:1623–33 CrossRef Medline